Indian Journal of Chemical Technology
Vol. 26, March 2019, pp. 122-130

Stable and microcrystalline Ce-Fe Bi-metal oxide nano particles: Synthesis, characterization and fluoride adsorption performance in drinking water

Adithya G T & Sivasankari C*

Department of Chemistry, Government College of Technology, Coimbatore 641 013, Tamil Nadu, India

E-mail: sivasankarigct@gmail.com

Received 21 November 2017; accepted 24 December 2018

The cerium-iron bi-metal oxide nano particles have been prepared as an adsorbent for the removal of fluoride from drinking water. The incorporated cerium ion into iron oxide is characterized using transition electron micrograph (TEM), X-ray diffraction (XRD) and Fourier transform infrared spectroscopy (FTIR), and morphologically observed by scanning electron microscope (SEM), energy dispersive X-ray (EDX) and Brunauer-Emmet-Teller surface area analyzer (BET). The effects of various factors such as solution *p*H, adsorbent dosage, equilibration time, initial fluoride ion concentration, water solubility and zero point charge have been investigated. The results show that the adsorbent removed about 98% of fluoride from drinking water at both acid and basic *p*H range, and the nano particles have extremely small size, high surface area, greater stability and microcrystalline nature. The experimental results suggest that this nano-adsorbent is promising for treating fluoride contaminated water.

Keywords: Nano particles, Adsorption, Bi-metal oxide, Fluoride, Co-precipitation

It is well-known that trace elements are essential and beneficial to the organism in minute concentrations, as they play a significant role in many metabolic processes. But they would be toxic when their concentrations exceed the limited levels. Fluoride, a typical trace element is distributed in rock, soil, and water. The safe limit of fluoride in drinking water level is in between 0.7 mg L^{-1} to 1.5 mg L^{-1} but harmful once it exceeds to 1.5 mg L^{-1} which is the World Health Organization limit being followed in most of the nation's[1]. Fluoride in minute quantity is an essential component for normal mineralization of bones and formation of dental enamel[2]. However, its excessive intake may result in slow, progressive crippling scourge known as fluorosis. It is endemic in at least 25 countries around the world and is most prevalent in India, China, and parts of Africa. It is not known how many people are now afflicted with the disease, but conservative estimates are in the tens of millions of people (WHO 2004). According to the WHO, at concentrations above 1.5 mg L^{-1}, fluoride is considered dangerous to human health. Excessive fluoride can lead to dental and skeletal fluorosis, a disease that can cause mottling of the teeth and calcification of ligaments. Long-term ingestion of fluoride-rich drinking water may show the way to crippling bone deformities, cancer, decreased cognitive ability, lower intelligence quotient, and developmental issues in children[3].

Excess fluoride in water, which could lead to serious health issues, has to be removed in a simple and economical way. The removal of fluoride from drinking water involves different methods such as adsorption, electrochemical treatment, coagulation/flocculation, membrane filtration, advanced oxidation technology, phytoextraction, electro-kinetic methods, electro-osmosis, and ion exchange. However, these methods have several disadvantages such as a high reagent need, unpredictable metal ion removal, and generation of toxic sludge. The adsorption process is very simple, economical, effective and versatile has become the most preferred methods for removal of fluoride from drinking water. This research work focuses on the removal of excess fluoride from drinking water using adsorption technique.

In the past ten years, many researchers have devoted attention to developing low-cost and effective nano-adsorbent for the removal of fluoride from aqueous solution and contaminated water. Various inorganic nano materials play a vital role in the removal of fluoride from aqueous solution. Among them, iron, alumina, titania, magnesia, silica, zirconium, cerium, and calcium-based metal oxide nano materials and composites play an important role

in defluoridation processes. These types of oxide nano materials are rich in surface functional groups, highly stable for adsorbing fluorides from aqueous solution. The increased surface areas of the metal oxide nano particles highly favour for fluoride adsorption. Their high adsorption capacity, non-toxic nature, limited solubility in water and good desorption potential makes metal oxides a material of choice[4]. Fluoride adsorption is determined by various factors such as the effect of contact time, adsorbent dosage, adsorbate concentration, *p*H and temperature.

In the previous report, Ce (IV)-doped iron oxide prepared by Yu Zhang *et al.*[5] with high ability to remove arsenic from water is of amorphous nature and Kankan *et al.*[6] with fluoride removal ability at *p*H 7. The endurance and stability of the adsorbent are improved since amorphous iron oxides have been effective for arsenic removal but it is not stable. In this present study, the prepared cerium-iron bi-metal oxide nano particles for fluoride removal are microcrystalline in nature, insoluble in water and hence it is stable and efficient. Further the prepared nano particles show efficient fluoride removal at all *p*H ranges from 2 to 10.

Experimental Section

Materials

Ferric chloride, ferrous sulphate, cerium sulphate, sodium fluoride and all other chemicals and reagents of analytical grade were purchased from Universal Scientific Co, Coimbatore. Fluoride stock solutions were prepared by dissolving 2.21 g of anhydrous sodium fluoride in 1000 mL distilled water in a plastic volumetric flask and all working solutions were prepared by appropriat dilution of stock solution with distilled water.

Synthesis of Ce-Fe bi-metal oxide nano particles

Co-precipitation technique was employed to synthesize Ce-Fe bi-metal oxide nano particles (CIBONs)[7]. $Ce(SO_4)_2.H_2O$ of 0.1 mol L^{-1} was dissolved in double distilled water together with 0.2 mol L^{-1} $FeCl_3.6H_2O$ and 0.1 mol L^{-1} $FeSO_4.7H_2O$ under gentle stirring, then 5 M NaOH solution was added until *p*H close to 10. Stirring was sustained for 60 min and rejuvenated for 4 h at room temperature. The suspension was repeatedly rinsed with distilled water till chloride and sulphate ions were entirely expelled. The prevailed sample was exsiccated at 110°C for 2 h. The exsiccated CIBONs was crushed and stored.

Instrumentation

Fluoride ion concentration was estimated by an expandable ion analyzer (Hach Meter, USA) with an ion selective fluoride electrode, and a fluoride ion selective electrode was calibrated prior to each experiment. The *p*H was measured with Elico LI 120 *p*H meter. The meter was calibrated whenever the measurements were made using *p*H calibration buffers. BET surface area was calculated using Quanta Chrome Nova-1000 surface analyzer instrument under liquid nitrogen temperature. FTIR spectra were recorded on a Shimadzu Prestige 20 IR Spectrometer in the range of 4000-400 cm^{-1} using KBr as a background. The high resolution transition electron microscope (HRTEM) images were taken using the JEOL JEM 2100 model with accelerating voltage of 200 kV model and elemental spectra were obtained using an Energy Dispersive X-ray spectroscopy (EDS) analyzer, the high resolution scanning electron microscope (HRSEM) images were taken using the Quanta 200 FEG model at 10 kV under pressure of $< 5.0 \times 10^{-3}$ Pa, the X-ray diffraction (XRD) measurements were obtained using a PAN analytical X'Pert Pro diffractometer model with the Cu Kα radiation ($\lambda = 1.54059^{o}$A) operated at 40 kV and 30 mA model and the Vibrating sample magnetometer (VSM) were recorded using a Lakeshore VSM 7410 model.

Batch experiments

With the predetermined quantity of CIBONs in 100 mL aqueous fluoride solution of desired initial concentration, taken in wide-mouth high-density polyethylene bottles of 250 mL capacity the batch experiments were mapped out. The fluoride solution was allowed to agitate in a mechanical shaker for a predetermined period till it reached the equilibration and the filtrate was analyzed for residual fluoride concentration. The effect of *p*H was performed by modifying the fluoride solution *p*H from 1.0-10.0 at an initial fluoride concentration of 10 mg L^{-1} and the CIBONs dose of 1.0 g L^{-1}. The effect of adsorbent dose was also studied by varying the adsorbent doses (0.1, 0.2, 0.3, 0.4, 0.5.....1.0 g L^{-1}) at an initial fluoride concentration of 10 mg L^{-1} and at optimum *p*H. Analyzing the percentage of fluoride removed by CIBONs at a time-honoured gap of 30 min for 6 h from 10 mg L^{-1} fluoride solution, the effect of contact time was evaluated. Equilibrium adsorption isotherms were drawn for fixed adsorbent dose and varying fluoride concentration from 10 mg L^{-1} to 100 mg L^{-1}

for 24 h contact time. The Erlenmeyer flask (250 mL) containing the known dosage of CIBONs with 100 mL of fluoride solution was placed on a mechanical shaker at room temperature (25±1°C) for a fixed time period. The flask was then removed and the solution was filtered. Each batch was repeated for three times and the mean value was taken for computation and to analyze the Temkin isotherm. All adsorption values were calculated from the change in solution concentration using the following equation.

$$Q_e = \frac{V(C_o - C_e)}{m} \quad \ldots (1)$$

where Q_e (mg/g) was the adsorbed quantity at equilibrium, C_o and C_e were the initial and final concentration (mg/L), V was the volume (L) taken and m was the mass of the adsorbent (g).

Sorption isotherms

Three commonly used isotherms namely Freundlich, Langmuir and Temkin had been adopted to quantify the CIBONs and the linear forms of three isotherms were represented in (Fig. 1-3) and the adsorption isotherm constants were tabulated in (Table 1).

In Table 1, Q_e was the quantity of fluoride adsorbed for each unit weight of the CIBONs (mg g^{-1}), C_e was the equilibrium concentration of the fluoride ion in the solution (mg L^{-1}), 1/n was the adsorption intensity and K_F was the Freundlich isotherm constant.

$$\log Q_e = \log K_F + \tfrac{1}{n} \log C_e \quad \ldots (2)$$

The linearized expression of the Freundlich model was represented by equation (2). The linear plot of log Q_e Vs log C_e indicated the applicability of the Freundlich isotherm for the CIBONs. The values of the 1/n between 0 and 1 and the n value with in the

Table 1 — Adsorption Isotherm Constents

Adsorption Isotherm	Isotherm Parameters	Numerical Values
Freundlich	K_F (mg g^{-1})	1.18
	1/n	0.5853
	n	1.71
	R^2	0.9728
Langmuir	Q_o	10.95
	K_L (mg g^{-1})	0.15
	R^2	0.9967
Temkin	K_T (mg g^{-1})	15.97
	B_T (kJ mol^{-1})	2.14
	R^2	0.9655

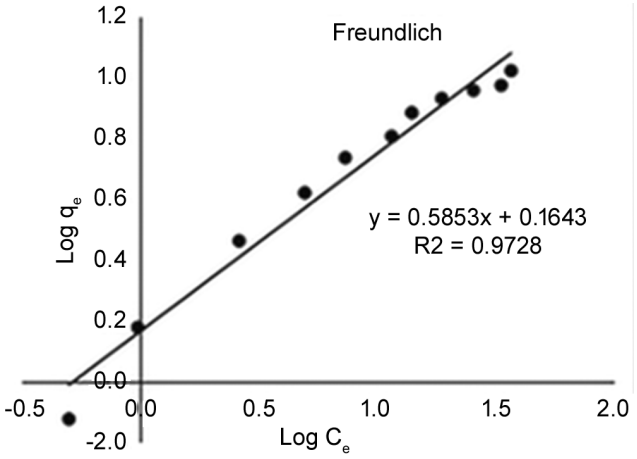

Fig. 1— Freundlich Isotherm of CIBONs (ranged left under figure)

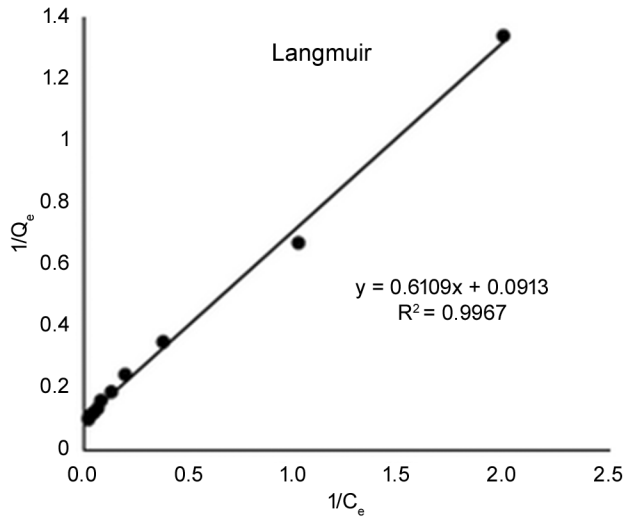

Fig. 2 — Langmuir Isotherm of CIBONs (ranged left under figure)

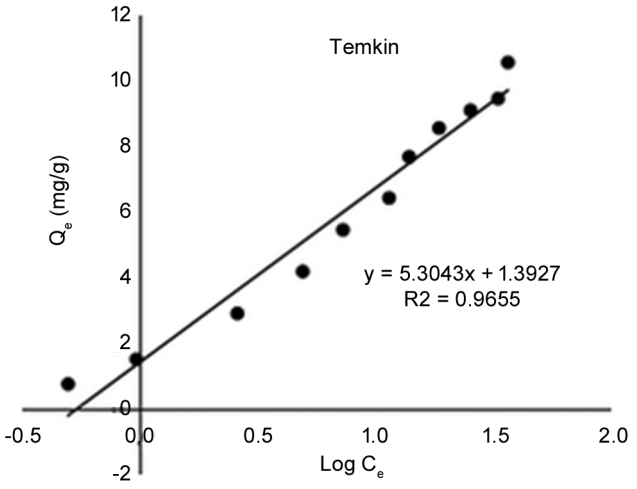

Fig. 3 — Temkin Isotherm of CIBONs (ranged left under figure)

range of 1-10 confirmed the conditions favourable for adsorption[8].

$$\frac{1}{Q_e} = \frac{1}{Q_o} + \frac{1}{K_L Q_o C_e} \quad \ldots (3)$$

In the Langmuir isotherm represented in equation (3), Q_o was the measure of adsorbate at complete mono layer coverage (mg g^{-1}) and bring about the maximum adsorption capacity of adsorbent and K_L (L mg^{-1}) was the Langmuir isotherm constant that related to the energy of adsorption of fluoride ions by the CIBONs. The Langmuir constants K_L and b for the CIBONs were calculated from the respective slope and the intercept of the plot C_e/Q_e Vs C_e respectively. The essential characteristics of the CIBONs' Langmuir isotherm can be enunciated in terms of a fundamental physical constant, a selectivity factor or an equilibrium constant[9].

$$Qe = \frac{RT}{B_T} \ln C_e + \frac{RT}{B_T} \ln K_T \quad \ldots (4)$$

Equation (4) represented the linearised expression for Temkin isotherm. This model depicted the fluoride ion and CIBONs interactions. The adsorption heat of all the molecules in the layer of the CIBONs decreases linearly with the coverage owing to fluoride ion-CIBONs interactions[10]. The value K_T (L g^{-1}) was the Temkin isotherm constant representing maximum binding energy of CIBONs, B_T (kJ mol^{-1}) was related to heat adsorption constant, R (8.314 kJ mol^{-1} K^{-1}) was the ideal gas constant and T was the temperature in Kelvin. The K_T value 15.97 confirmed the interaction between F^- and CIBONs and B_T value 2.14 showed a small variation in the heat of adsorption. The R^2 value was close to one confirming the suitability of this model that resulted in the size decrease.

Results and Discussion

BET Surface area analysis

The surface area, pore volume and pore diameter were considerable factors to influence the adsorption property of the adsorbent. The same for cerium oxide and iron oxide were enumerated and listed in (Table 2) were 9.5 m^2/g, 0.01 cm^3/g and 2.5 nm and 5.91 m^2/g, 0.007 cm^3/g and 3.53 nm, respectively. In comparison with cerium oxide and iron oxide, the surface area, pore volume and pore diameter of CIBONs increased to 90.5 m^2/g, 0.092 cm^3/g and 1.19 nm respectively. The increase in surface area was due to the incorporation of iron oxide into the trace of cerium ion.

Fourier Transform Infrared Spectroscopy analysis

The Fourier transform infrared spectroscopy (FTIR) spectra were exhibited in (Figs 4 and 5). The CIBONs was mixed with spectroscopic grade KBr and analyzed. The band at 3414.15 cm^{-1} was

Table 2 — BET Surface Area Analysis of prepared cerium oxide nano particles, iron oxide nano particles and CIBONs

	Surface Area (m^2/g)	Pore Volume (cm^3/g)	Pore Diameter nm
Cerium Oxide Nanoparticles	9.5	0.01	2.5
Iron Oxide Nanoparticles	5.91	0.007	3.53
CIBONs	90.5	0.092	1.19

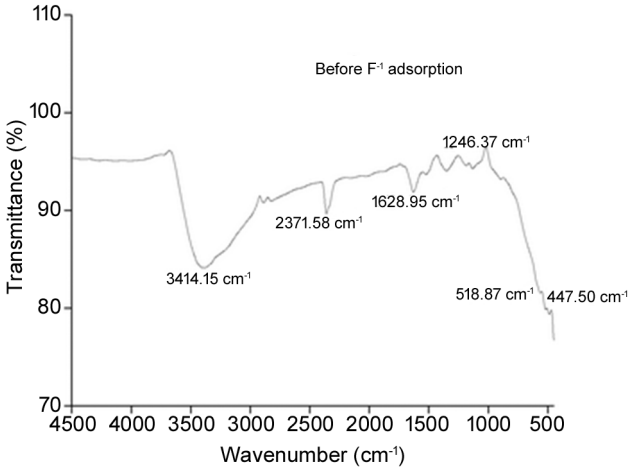

Fig. 4 — FTIR spectrum of CIBONs before fluoride adsorption

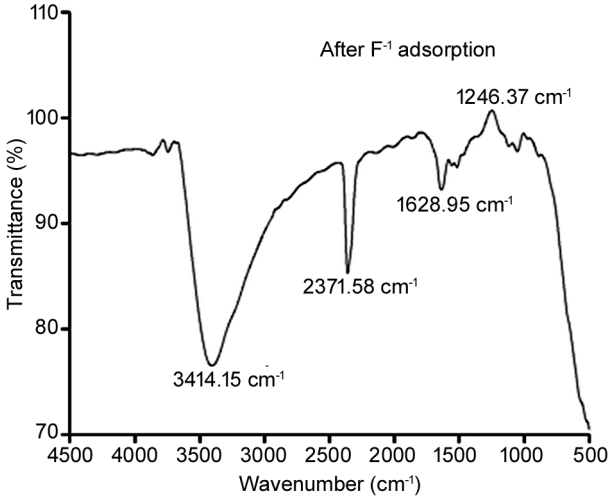

Fig. 5 — FTIR spectrum of CIBONs after fluoride adsorption

attributed to the stretching vibration of hydroxyl radical (-OH)[11]. The band at 2371.58 cm^{-1} was attributed to the Ce-O vibration [12]. The band at 1628.95 cm^{-1} was due to the bending vibration of interlayer water molecules[13]. The band at 1246.37 cm^{-1} was attributed to the bending vibration of the metal hydroxide (M-OH)[14], and the decrease of the integral area of M-OH was observed after removal. The results justified the participation of hydroxyl group in the adsorption of fluoride. The band at 518.87 cm^{-1} and 447.50 cm^{-1} were attributed to the Fe-O bending vibration[8,15]. The emergence of a band near 400 cm^{-1} in (Fig. 5) attributed the metal fluoride vibrations[16], and implied the binding ability of fluoride ion with the surface of CIBONs after adsorption.

X-Ray Powder Diffraction analysis

The X-ray powder diffraction (XRD) scanning was carried out from 5^o to 90^o (2θ) at a scan rate of 10^o/min and was looked over using software assigned to the instrument. The peaks displayed in Figs 6 and 7 featured the patterns of iron oxide and cerium oxide that was prepared in the same way as CIBONs were prepared. The pattern in Fig. 6 corresponded to the Fe_3O_4[17] (JCPDS card No. 01-089-6466) and the pattern in Fig. 7 corresponded to the CeO_2 (JCPDS card No. 00-023)[18]. The peaks in Fig. 8 displayed the CIBONs featuring microcrystalline peaks that were absolutely different from those patterns found in iron oxide and cerium oxide, indicating a new phase structure of CIBONs.

Morphological analysis

The high-resolution scanning electron microscope (HRSEM) images of CIBONs were shown in the Fig. 9. The CIBONs were found to possess spherical and agglomerated morphology.

The spherical and agglomerated morphology of CIBONs was further verified by high resolution transition electron microscope (HRTEM). The HRTEM images of CIBONs before and after fluoride adsorption were shown in Figs 10 and 11. The Energy Dispersive X-ray Spectroscopy (EDS) mapping was done using an Energy Dispersive X-ray Spectroscopy (EDS) analyzer before and after fluoride adsorption and shown in Figs 12 and 13. From Fig. 13, the peak for the F^- was seen, signifying that F^- was occupied by the CIBONs. In addition, the EDS mapping contributed a direct elemental distribution on the surfaces of CIBONs, and the microcrystalline morphology was not altered even after fluoride adsorption. The EDS also justified the atomic ratio of the Fe/Ce contained in the CIBONs was nearly 3/1. This result concurred with the

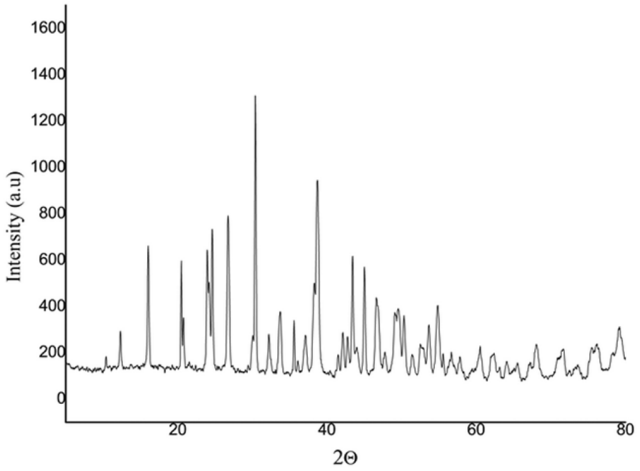

Fig. 7 — *XRD pattern of cerium oxide*

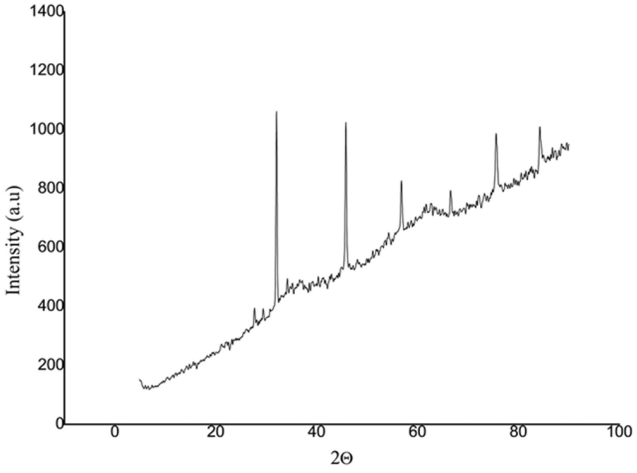

Fig. 6 — XRD pattern of iron oxide

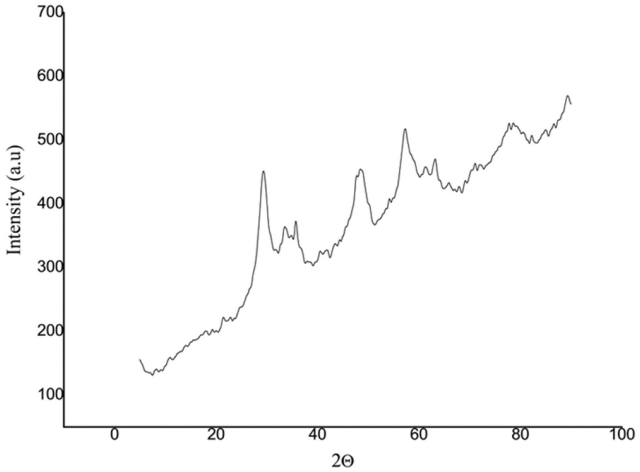

Fig. 8 — *XRD pattern of CIBONs*

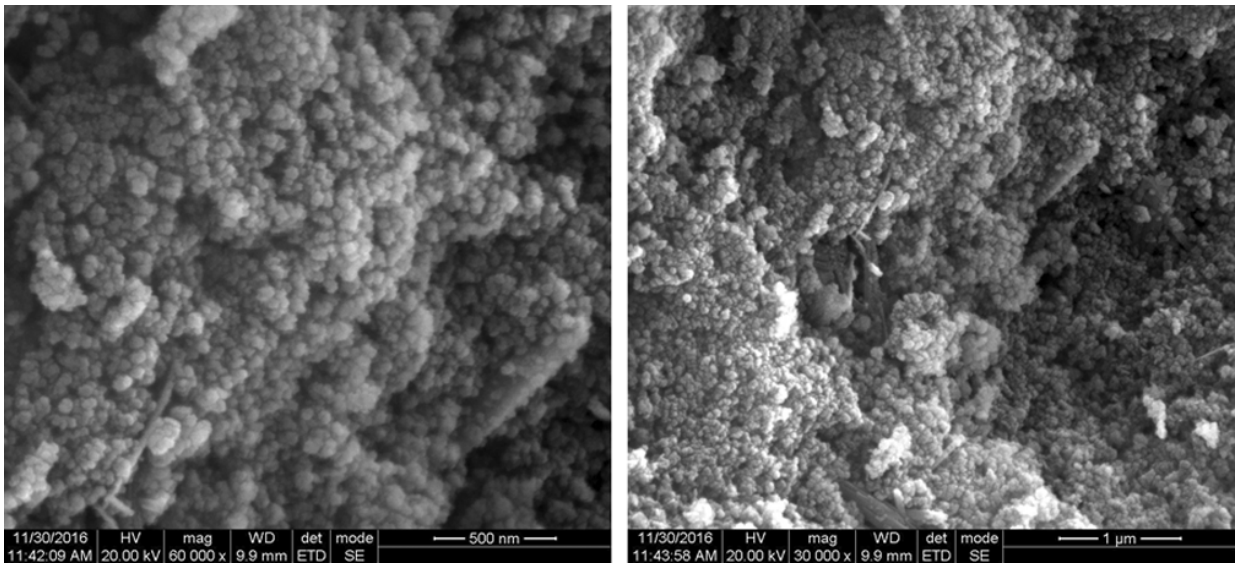

Fig. 9 — HRSEM images of CIBONs

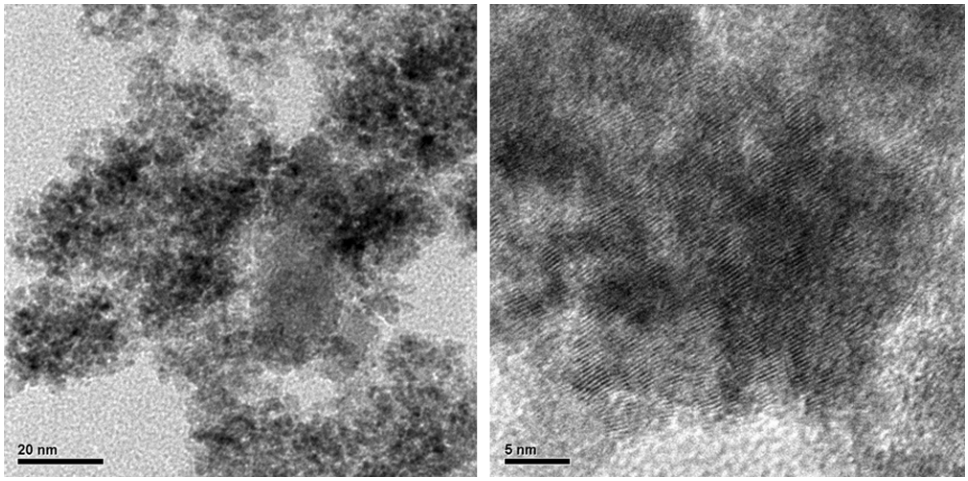

Fig. 10 — HRTEM images of CIBONs before fluoride adsorption

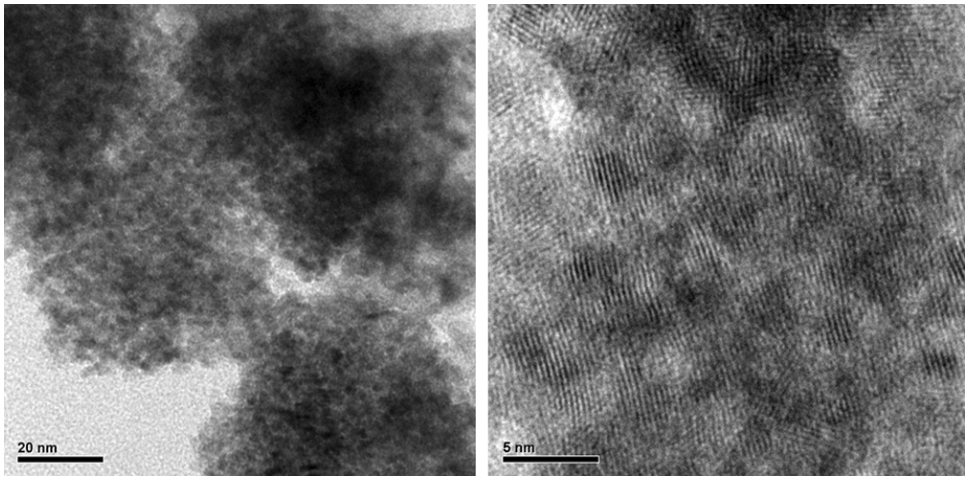

Fig. 11— HRTEM images of CIBONs after fluoride adsorption

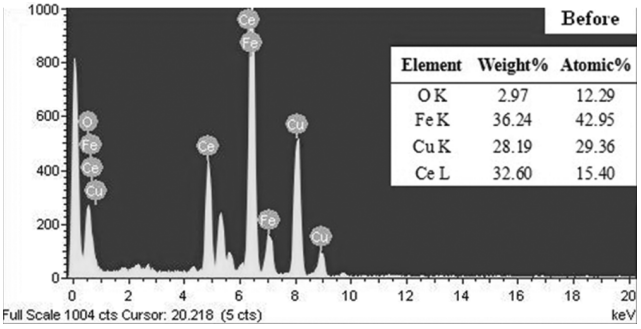

Fig. 12 — EDS image of CIBONs before fluoride adsorption

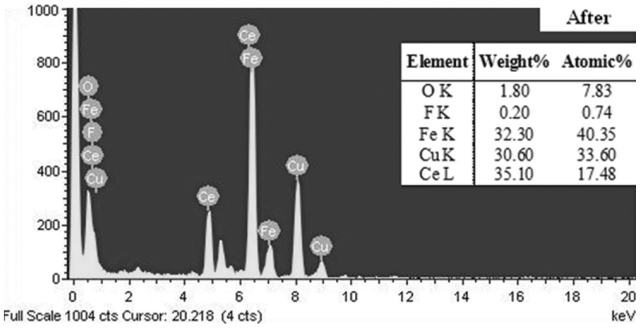

Fig. 13 — EDS image of CIBONs after fluoride adsorption

initial Fe/Ce molar ratio, justifying that cerium and iron were entirely packed on the CIBONs.

Vibrating sample magnetometer analysis

Figure 14 displayed the magnetization curve as a function of magnetic field (G) for the CIBONs. The VSM result revealed that the CIBONs were ferromagnetic in nature with a coercivity and a saturation magnetization of 115.10 G and 38.331 emu g^{-1} [19].

Effect of adsorbent dosage on fluoride removal

The various adsorbent dosages from 0.1 to 1 g under room temperature were habituated to investigate the effect of adsorbent dosages on the fluoride expulsion. The obtained results were shown in Fig. 15. As exhibited in Fig. 15 the excessive quantity of fluoride was consumed when CIBONs dosage raised from 0.4 to 1 g from 83% to 97%, suggesting that the adsorption process reached a dynamic equilibrium due to enough active adsorption sites for the binding of fluoride ions at higher adsorbent dosages.

Effect of *p*H

The *p*H of the aqueous solution was one of the key limits which mostly affect the fluoride adsorption.

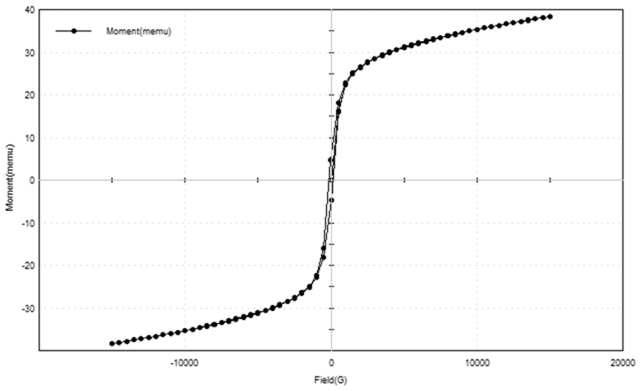

Fig. 14 — VSM image of CIBONs

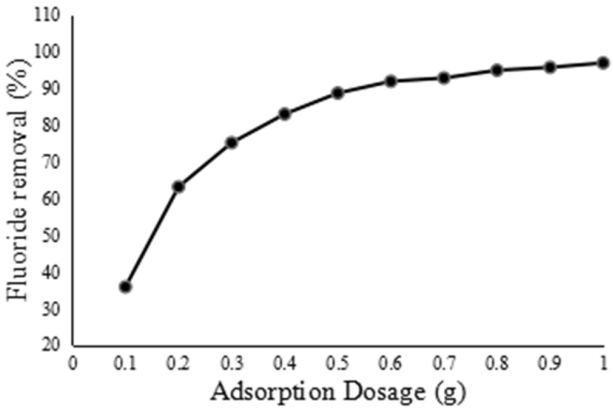

Fig. 15 — Effect of adsorbent dosage

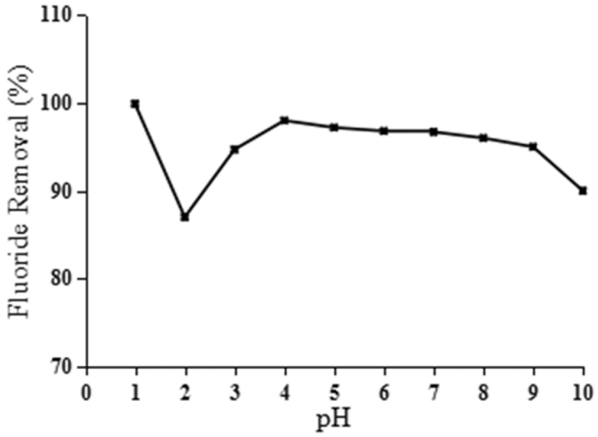

Fig. 16 — Effect of pH

Figure 16 represented the effect of *p*H value of aqueous solution on the capacity of the CIBONs. The maximum adsorption capacities were noted at all *p*H values. It is evident that the removal was over 99% at *p*H below 2.0. However, it was found that the removal of fluoride was around 98% by CIBONs in the *p*H range 3.0 - 9.0. It was also observed that the fluoride

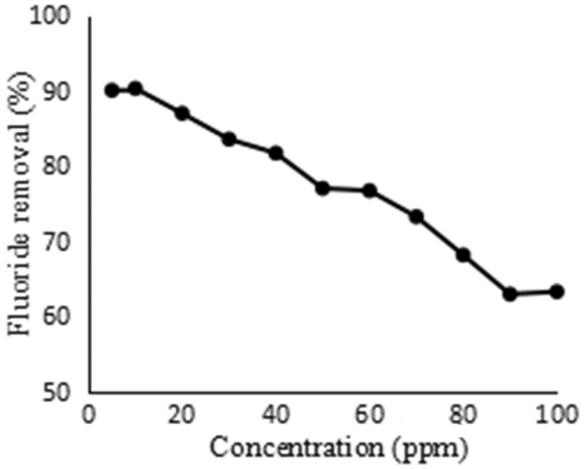

Fig. 17 — Effect of initial fluoride concentration

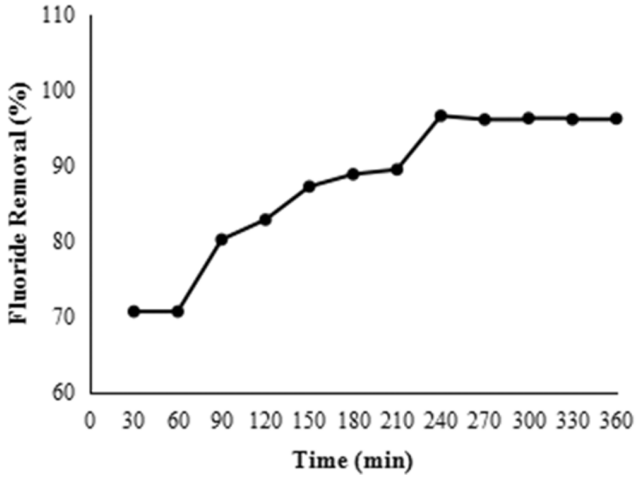

Fig. 18 — Effect of contact time

removal was drastically reduced to 91.8% due to electrostatic repulsion of fluoride ion with the CIBONs. Hence, an optimum *p*H of 6.5±0.5 was maintained for further studies. In addition the zero point charge (*p*Hpzc) of CIBONs was found to be 7.3, this meant that the surface charge of CIBONs was positive when *p*H < 7.3 and by electrostatic interaction F^- got attracted to the positively charged CIBONs and got a negative charge at a solution *p*H higher than 7.3 so that the hydroxyl ion will get replaced by fluoride ion.

Effect of initial fluoride concentration

The initial fluoride concentration was the driving force for the fluoride mass transfer from the aqueous solution to CIBONs. The effect of the initial fluoride concentration (from 5 to 10 mg L^{-1}) on the adsorption capacities of CIBONs was evaluated at *p*H 6.5±0.5 under room temperature with 1 g L^{-1} of CIBONs. The obtained results are presented in Fig. 17. It showed that the percent removal of fluoride decreased with increase in concentration.

Effect of contact time

The effect of contact time on the fluoride adsorption onto CIBONs was investigated. Figure 18 showed the progression of adsorption reaction and the percent removal of fluoride for different contact times. As shown in Fig. 18, the removal of fluoride increased with time and attained an equilibrium value of 98% after 240 min.

Regeneration of CIBONs

To regenerate the CIBONs from fluoride ion, trial the run was were performed with dilute solutions of HCl, H_2SO_4 and $Al_2(SO_4)_3$ as a regenerant[20]. The effective regeneration of the CIBONs was brought using aluminium sulphate solution. A series of adsorption experiments were conducted with 100 mL of 10 mg L^{-1} fluoride solution containing 1.0 g of CIBONs at an optimum *p*H of 6.5 ± 0.5 and a contact time of 4 h. At the end of the period, the fluoride content of the supernatant solution was established. The CIBONs was separated quantitatively, washed several times with distilled water to remove any unadsorbed fluoride ions.

Aluminum sulphate solution of volume 100 mL and concentration varying from 0.05-5.0% w added to each of these fluoride loaded CIBONs samples and agitated for 4 h. At the end of this period, the samples were washed several times with distilled water to remove excess aluminum (III) ions. Adsorption studies were conducted using each of these regenerated CIBONs to find out the fluoride removal capacity. The regenerated CIBONs were found to retain the same fluoride removal capacity after regeneration. From the study, it was concluded that at least 100 mL of 0.25% aluminum sulphate solution is required for the complete regeneration of 1.0 g of CIBONs.

Conclusion

The iron oxide was incorporated in a trace of cerium oxide in a simple way and the water insoluble, ferromagnetic and microcrystalline CIBONs with agglomerated spherical structure were successfully prepared using co-precipitation method. The incorporated cerium ion into iron oxide had an effective response to the surface area increase and the removal percentage of fluoride in the entire *p*H range.

The maximum fluoride removal was observed at *p*H ranges of 3.0-9.0 indicating that the adsorbent has promising potential utility in drinking water processes. The CIBONs well-suited for Langmuir adsorption than Freundlich implying the mono layer adsorption of fluoride. Kinetic study results indicated that the adsorption process followed pseudo–second order kinetics. The adsorption capacity of fluoride on the surface of CIBONs was found to be 10.95 mg g^{-1} at *p*H 6.5 ± 0.5. The CIBONs regeneration was carried out using aluminium sulphate. The laboratory results suggested that the CIBONs was favourable adsorbent for treating fluoride contaminated drinking water.

Acknowledgement

The authors thank the partial financial support from TEQIP Phase II and members of the Department of Chemistry, Government College of Technology, Coimbatore, and we acknowledge the technical support of SAIF-IITM for SEM analysis, PSG Institute of Advance Science and Research for TEM analysis, DRDO-Bharathiyar University Center for Life Sciences for XRD and FTIR analysis and Bangalore Institute of Technology for BET surface area analysis.

References

1 Fawell J, Bailey K, Chilton J, Dahi E, Fewtrell L & Magara Y, *Fluoride in Drinking Water*, WHO, 2006.

2 Bell M C & Ludwig T G, *The Supply of Fluoride to Man: Ingestion from Water, in: Fluorides and Human Health*. WHO Monograph Series 59, WHO, 1970.

3 Vithange Methika & Bhattacharya Prosun. *Fluoride in Drinking Water: Health Effects and Remediation; CO_2 Sequestration, Biofuels and Depollution*, 5 (2015) 105.

4 Suriyaraj S P & Sevakumar R, *RSC Adv*, 6 (2016) 10565.

5 Yu Zhang, Min Yang & Xia Huang, *Chemosphere*, 51(2003) 945.

6 Kankan Mukhopadhyay, Abir Ghosh, Supriyo Kumar Das, Bibhutibhushan Show, Palani Sasikumar &Uday Chand Ghosh, *RSC Adv*, 7 (2017) 26037.

7 Kandpal N D, Sah N, Loshali R, Joshi R & Prasad J, *J Sci Ind Res,* 73 (2013) 87.

8 Goswami A & Purkait M K, *J Water Proc Eng*, 1 (2014) 91.

9 Naicai Xu, Zhong Liu, Yaping Dong, Tianzeng Hong, Li Dang & Wu Li, *Ceram Int*, 2016.

10 Imran Ali, Zeid A, Alothman & Mohd Marsin Sanagi, *J Mol Liq*, 211(2015) 457.

11 Sairam Sundaram C, Natrayasamy Viswanathan & Meenakshi S, *J Hazard Mater*, 155(2008) 206.

12 Ghosh Abir, Chakrabarti sharadindra, Biswas Krishna & Ghosh Uday Chand, *Appl Surf Sci*, 307 (2014) 665.

13 Biswas Krishna, Gupta Kaushik & Ghosh Uday Chand, 149 (2008)196.

14 Subbaiah Muthu Prabhu & Sankaran Meenakshi, *Carbohydr Polym*, 120 (2015) 60.

15 Babu C M, Palanisamy B, Sundaravel, Palanichamy M & Murugesan V, *J Nanosci Nanotechnol*, 13 (2013) 2517.

16 Gima W Woyessa, Srivastava B B L & Ephrem G Demissie, *Int J Sci Eng Res*, (2014) 5.

17 Agarwal1 T, Gupta K A, Alam S & Zaidi M G H, *Int J Compos Mater*, 2 (2012) 17.

18 Ming Ge, Changsheng Guo, Lei Li, Baoquan Zhang, Yinchang Feng& Yuqiu Wang, *Mater Lett*, 63 (2009) 1269.

19 Bryan D Korth, Pei Keng,Inbo Shim, Steven E Bowles, Chuanbing Tang, Tomasz Kowalewski, Kenneth W Nebesny & Jeffrey Pyun, *J Am Chem Soc*, 128 (2006) 6562.

20 Sivasankari C & Arulanandham A*, Ind J Chem Technol,* 21(2014) 70.